APPLICATION OF NUMERICAL METHODOLOGIES IN THE DYNAMIC ANALYSIS OF HYDROGENERATORS

Felipe J. Vinaud[1]
Alberto C.G.C. Diniz[2]
Universidade de Brasília - UnB
Campus Universitário Darcy Ribeiro
Brasília - DF - Brasil CEP 70910-900
1 - fvinaud@unb.br
2 - adiniz@unb.br

Abstract. *The purpose of this work is the use of simplified models in the rotordynamic analysis of a hydroelectric rotor-generator assembly. The analysis of different methodologies will allow for acquaintance with a phonomenological sense of the runing conditions of the assembly. Thus, the methodology will enable the detection of unstable vibrations and suply a control parameter to be used in more complex simulations. The Rayleigh-Ritz and Finite Element Methodologies are employed and produced results on which it is possible to locate critical speeds. The preliminar model to be simulated is a simplified reproduction of the working conditions at the Coaracy Nunes power plant under Eletronorte administration.*

Keywords:*hydrogenerator, Rayleigh-Ritz, Finite Elements, frequency response, time history behavior.*

1. Introduction

During recent years it has been observed an increase in the demand for electrical power . Thus, a more efficient genertation of power is to be assessed in order to optimize the operation of old hydro power plants and increase the extraction of energy from the water. With this aim, this work was proposed as a preliminar study of the running conditions of rotor-generator assemblies such as the Coaracy Nunes assembly in a rotordynamic standpoint.

This article presents a simple study of the Rayleigh-Ritz and Finite Element methodologies and their use in an adapted model of the assembly under study. Both methodologies allow the calculation of the general behaviour of the assembly.

The Rayleigh-Ritz methodolgy was used with the intent of achieving a description of such behaviour using few degrees of freedom allowing the understanding of the physical phenomena involved. One of these phenomena is the evolution of the lower natural frequencies of the system with the increase of rotational speed. The Finite Element formulation makes possible a more practical description of such phenomena due to the possibilities of its use in large scale problems.

2. The Rayleigh-Ritz methodology

The rotor-generator assembly being modeled in this work is comprised of two discs, one shaft and two bearings. For the use of the Rayleigh-Ritz methodology the energy equations of each component is needed (Lalanne, 1996). The unbalance, which cannot be completely avoided, needs to be taken into account as well. Figure 1 depicts the modeled assembly.

The kinetic energy expressions are used for the discs, shaft and unbalance models. The strain energy is used in the shaft model. Bearings are represented by the virtual work exerted on the shaft. Hence, the movement equations of a rotor are attained by the insertion of those energy expressions in Lagrange's equation:

$$\frac{d}{dt}\left(\frac{\partial T}{\partial \dot{q_i}}\right) - \frac{\partial T}{\partial q_i} + \frac{\partial U}{\partial q_i} = Fq_i \quad (1 \leq i \leq N) \tag{1}$$

where N is the number of degrees of freedom, q_i are the independent generalized coordinates and Fq_i are the generalized forces.

2.1 The discs

The discs are regarded as rigid strctures and can be represented by their kinetic energy. The kinetic energy of one disc is attained by its rotation around its center of mass and is calculated through displacement variables relating a coordinate system fixed on the disc and rotating with it and a fixed reference coordinate system. In the reference coordinate system, u and w are the coordinates of the centre of mass along the X and Z axes respectively. The angles θ and ψ are the angles of rotation relating the inclination of the disc with respect to the reference coordinate system. The kinetic energy is expressed finally, for each disc, by:

$$T_d = \frac{1}{2}M_d\left((\dot{u})^2 + (\dot{w})^2\right) + \frac{1}{2}I_{dx}\left((\dot{\theta})^2 + (\dot{\psi})^2\right) + \frac{1}{2}I_{dy}\left(\Omega^2 + 2\Omega\dot{\psi}\theta\right) \tag{2}$$
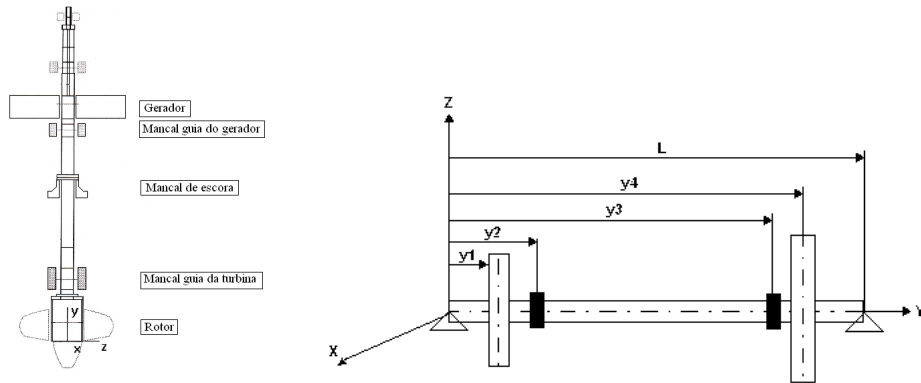
Figure 1. Modeled assembly

where the term $\frac{1}{2}I_{dy}\Omega^2$ represents the kinetic energy of the disc rotating at an angular speed Ω. This term is constant and will not modify the equations of motion in Eq. (1). The term $I_{dy}\Omega\dot{\psi}\theta$ represents the gyroscopic effect.

2.2 The shaft

The kinetic energy expression for the shaft is an extension of that obtained for the discs. For an element of length L and constant cross section the kinetic energy expression is:

$$T_s = \frac{\rho S}{2}\int_0^L \left((\dot{u})^2 + (\dot{w})^2\right)dy + \frac{\rho I}{2}\int_0^L \left((\dot{\psi})^2 + (\dot{\theta})^2\right)dy + \rho IL\Omega^2 + 2\rho I\Omega\int_0^L \dot{\psi}\theta dy \qquad (3)$$

where ρ is the density, S the cross-sectional area and I the moment of inertia of the shaft. The first integral represents the classical problem of a beam under bending. The second integral represents the effects of rotational inertia. The term $\rho IL\Omega^2$ is constant and will not influence the equations of motion.

For obtaining the strain energy, it is necessary to consider a point $B(x, y)$ in the cross-section of the beam. A coordinate system fixed to the shaft, and thus rotating with it, is considered. u^* and w^* are the coordinates of the geometric centre of the cross section with respect to the rotating axes x and z respectively. The strain energy of point B in the cross section of the disc is calculated in the rotating coordinate system and second order terms are neglected. The stress-strain relationship and coordinate system transformations such as $u^* = u\cos\Omega t - w\sin\Omega t$ and $w^* = u\sin\Omega t - w\cos\Omega t$ must be used. The diametral moments of inertia in the x and z directions have to be inserted as well. After some calculations, one can obtain an expression for the strain energy in the reference coordinate system which can be simplified by the assumption of a symmetric shaft ($I = I_x = I_z$). Thus, the strain energy is:

$$U_s = \frac{EI}{2}\int_0^L \left[\left(\frac{\partial^2 u}{\partial y^2} + \frac{\partial^2 w}{\partial y^2}\right)^2\right] \qquad (4)$$

2.3 Bearings

The bearing properties are supposed known. Thus, the virtual work δW of the external forces acting on the shaft is found for each bearing in the compact form $\delta W = F_u\delta u + F_w\delta w$. F_u and F_w are the generalized force components and take into account the stiffness and damping coefficients assumed for the bearings in question. They can be expressed in the matricial form as:

$$\left[\begin{array}{c} F_u \\ F_w \end{array}\right] = -\left[\begin{array}{cc} k_{xx} & k_{xz} \\ k_{zx} & k_{zz} \end{array}\right]\left[\begin{array}{c} u \\ w \end{array}\right] - \left[\begin{array}{cc} c_{xx} & c_{xz} \\ c_{zx} & c_{zz} \end{array}\right]\left[\begin{array}{c} \dot{u} \\ \dot{w} \end{array}\right] \qquad (5)$$

2.4 The unbalance

The unbalance is due to a mass m_u located at a distance d from the geometric centre of the shaft and its kinetic energy is to be calculated. The mass is located on a perpendicular plane with respect to the y shaft and its coordinate with respect to y is constant. The angular displacement is Ωt. In the reference coordinate system, the kinetic energy is given by:

$$T_u = \frac{m_u}{2}\left[(\dot{u})^2 + (\dot{w})^2 + \Omega^2 d^2 + 2\Omega\dot{u}d\cos\Omega t - 2\Omega\dot{w}d\sin\Omega t\right] \qquad (6)$$

The term $m_u\Omega^2 d^2/2$ is constant and will not modify the equations of motion. The mass m_u is a different measure for each disc and, hence, the kinetic energy can be simplified as in:

$$T_b \approx m_b\Omega d(\dot{u}\cos\Omega t - \dot{w}\sin\Omega t) \qquad (7)$$

2.5 Equations of motion

The Rayleigh-Ritz method is characterized by the replacement of displacements u and w by two functions: one time dependent generalized coordinate $q_i(t)$ and one displacement function $f(y)$ depending on the coordinate y along the shaft representing the shape of the first vibration mode of a simply supported beam. Hence, u, w and their time derivatives can be expressed as in Eqs. (8) and (9) and angles θ and ψ, supposed small, as in Eq. (10) :

$$u = f(y)q_1, \qquad w = f(y)q_2, \qquad \dot{u} = f(y)\dot{q}_1, \qquad \dot{w} = f(y)\dot{q}_2 \tag{8}$$

$$f(y) = \sin\frac{\pi y}{L}, \qquad \frac{df(y)}{dy} = g(y) = \frac{\pi}{L}\cos\frac{\pi y}{L} \tag{9}$$

$$\theta = \frac{\partial w}{\partial y} = \frac{df(y)}{dy}q_2 = g(y)q_2, \qquad \psi = -\frac{\partial u}{\partial y} = -\frac{df(y)}{dy}q_1 = -g(y)q_1 \tag{10}$$

The displacements and angles can be replaced in the energy expressions for the calculation of the global energy expressions. The global kinetic energy, resulting from the sum of all the kinetic energies of the system can be writen as in Eq. (11):

$$T = A\left(\dot{q}_1^2 + \dot{q}_2^2\right) + B\left(\dot{q}_1 q_2\right) + C\left(\dot{q}_1\cos\Omega t - \dot{q}_2\sin\Omega t\right) \tag{11}$$

where A, B and C are respectively:

$$A = \frac{1}{2}\left[M_{d1}f(y_1)^2 + M_{d2}f(y_4)^2 + Ix_{d1}g(y_1)^2 + Ix_{d2}g(y_4)^2 + \rho SL + \frac{\pi\rho I_a}{4L}\right] \tag{12}$$

$$B = \Omega\left[Iy_{d1}g(y_1)^2 + Iy_{d2}g(y_4)^2 + \rho I_a L\pi\right], \qquad C = \Omega\left[m_{b1}d_1 f(y_1) + m_{b2}d_2 f(y_4)\right] \tag{13}$$

The global strain energy is expressed by the strain energy of the shaft as in Eq. (4):

$$U = \frac{\pi E I_a}{4}\left(\frac{\pi}{L}\right)^3\left(q_1^2 + q_2^2\right) \tag{14}$$

The virtual work is calculated as the sum of the virtual works exerted by the two bearings on the shaft. It is also considered the simetry of cross coupling terms ($k_{xz} = k_{zx}$ and $c_{xz} = c_{zx}$). The generalized forces obtained are:

$$\begin{bmatrix} F_u \\ F_w \end{bmatrix} = -\begin{bmatrix} k_{xx1}f(y_1)^2 + k_{xx2}f(y_2)^2 & k_{xz1}f(y_1)^2 + k_{xz2}f(y_2)^2 \\ k_{zx1}f(y_1)^2 + k_{zx2}f(y_2)^2 & k_{zz1}f(y_1)^2 + k_{zz2}f(y_2)^2 \end{bmatrix}\begin{bmatrix} q_1 \\ q_2 \end{bmatrix}$$
$$-\begin{bmatrix} c_{xx1}f(y_1)^2 + c_{xx2}f(y_2)^2 & c_{xz1}f(y_1)^2 + c_{xz2}f(y_2)^2 \\ c_{zx1}f(y_1)^2 + c_{zx2}f(y_2)^2 & c_{zz1}f(y_1)^2 + c_{zz2}f(y_2)^2 \end{bmatrix}\begin{bmatrix} \dot{q}_1 \\ \dot{q}_2 \end{bmatrix} \tag{15}$$

indexes 1 and 2 represent bearings 1 and 2. More bearings can be added to the system by the same manner.

The system equations of motion are obtained by plugging the energy expressions into Lagrange's equation and solving for the time derivatives of the generalized displacements:

$$2A\ddot{q}_1 + \frac{B}{\Omega}\Omega\dot{q}_2 + \frac{\pi^4 E I_a}{2L^3}q_1 = C\Omega\sin\Omega t \tag{16}$$

$$2A\ddot{q}_2 - \frac{B}{\Omega}\Omega\dot{q}_1 + \frac{\pi^4 E I_a}{2L^3}q_2 = C\Omega\cos\Omega t \tag{17}$$

If one is to analyze the non-forced behaviour of the system, then the homogeneous equations are:

$$M_{eq}\ddot{q}_1 + C_{eq}\Omega\dot{q}_2 + K_{eq}q_1 = 0 \tag{18}$$

$$M_{eq}\ddot{q}_2 - C_{eq}\Omega\dot{q}_1 + K_{eq}q_2 = 0 \tag{19}$$

with $M_{eq} = 2A$, $C_{eq} = B/\Omega$ and $K_{eq} = \pi^4 E I_a/(2L^3)$. Initial conditions are used in the integration of the equations of motion allowing one to attain the precession orbits of the shaft. Depending on the inital conditions, it is possible to obtain forward or backward whirling orbits.

Natural frequencies are obtained assuming a solution such as $q_1 = Q_1 e^{rt}$ and $q_2 = Q_2 e^{rt}$ and using it in Eqs. (18) and (19) leading to a system of homogeneous equations. The non-trivial solution of such system will lead to the following characteristic equation:

$$M_{eq}r^4 + (2M_{eq}K_{eq} + C_{eq}^2\Omega^2)r^2 + K_{eq}^2 = 0 \tag{20}$$

When $\Omega = 0$ (static rotor) the solution to Eq. (20) is:

$$r_{1stat}^2 = r_{2stat}^2 = j^2\omega_{1stat}^2 = j^2\omega_{2stat}^2 = -\frac{K_{eq}}{M_{eq}} \tag{21}$$

with $j^2 = -1$. The frequencies are: $\omega_{1stat} = \omega_{2stat} = \sqrt{K_{eq}/M_{eq}}$. When the system is under rotation, roots r_1 and r_2 and the corresponding frequencies are:

$$r_1^2 = j^2\omega_1^2, \quad \omega_1 = \sqrt{\omega_{1stat}^2 + \frac{C_{eq}^2\Omega^2}{2M_{eq}^2}\left(1 - \sqrt{1 + \frac{4M_{eq}^2\omega_{1stat}^2}{C_{eq}^2}\Omega^2}\right)} \tag{22}$$

$$r_2^2 = j^2\omega_2^2, \quad \omega_2 = \sqrt{\omega_{1stat}^2 + \frac{C_{eq}^2\Omega^2}{2M_{eq}^2}\left(1 + \sqrt{1 + \frac{4M_{eq}^2\omega_{1stat}^2}{C_{eq}^2}\Omega^2}\right)} \tag{23}$$

Equations (22) and (23) show the evolution of the natural frequencies of modes 1 and 2 as the rotation speed increases. With those equations it is possible to build the Campbell diagram that will indicate critical rotational speeds of the system (speeds that coincide with natural frequencies causing resonance).

3. The Finite Element method

The basis for the Finite Element system matrices are the matrices obtained for the shaft. Elements such as discs and bearings are added to the shaft matrices in order to build the system matrices. In this problem, some important assumptions have to be made: there are no displacements in the y direction; angles and displacements are considered to be small; gyroscopic effects will happen only around the y direction; angles around the x and z directions are much smaller than Ω; plane cross-sections remain plane after deformation; element displacements are represented by Hermitian shape functions.

Discs and bearings are concentrated at nodal positions. This means that their behavior is be added to the system matrices in specific nodal positions and this is done after the shaft matrices are built.

3.1 Discs

Each node possesses four degrees of freedom: two displacements u and w and two angles θ and ψ. The δ vector of nodal displacements of the centre of the disc is $\delta = [u, w, \theta, \psi]^t$. The use of Eq. (2) into Lagrange's equation leads to:

$$\frac{d}{dt}\left(\frac{\partial T}{\partial \dot{\delta}}\right) - \frac{\partial T}{\partial \delta} = \begin{bmatrix} M_d & 0 & 0 & 0 \\ 0 & M_d & 0 & 0 \\ 0 & 0 & I_{dx} & 0 \\ 0 & 0 & 0 & I_{dx} \end{bmatrix} \begin{Bmatrix} \ddot{u} \\ \ddot{w} \\ \ddot{\theta} \\ \ddot{\psi} \end{Bmatrix} + \Omega \begin{bmatrix} 0 & 0 & 0 & 0 \\ 0 & 0 & 0 & 0 \\ 0 & 0 & 0 & -I_{dy} \\ 0 & 0 & I_{dy} & 0 \end{bmatrix} \begin{Bmatrix} \dot{u} \\ \dot{w} \\ \dot{\theta} \\ \dot{\psi} \end{Bmatrix} \tag{24}$$

where the first matrix is the mass matrix and the second matrix a gyroscopic matrix.

3.2 Shaft

The shaft is modelled as a beam with circular cross-section. Each element has two nodes and eight degrees of freedom. Thus, the elementary matrices have eight degrees of freedom on its span. The relations between angles and displacements are $\theta = \frac{\partial w}{\partial y}$ and $\psi = -\frac{\partial u}{\partial y}$.

The nodal displacement vector is $\delta = [u_1, w_1, \theta_1, \psi_1, u_2, w_2, \theta_2, \psi_2]^t$, which can be split into two vectors:

$$\delta u = [u_1, w_1, \theta_1, \psi_1]^t \quad \text{and} \quad \delta w = [u_2, w_2, \theta_2, \psi_2]^t \tag{25}$$

Displacements u and w can be expressed as functions of the hermitian shape functions ($N_i(y)$) and nodal displacements δu and δw as in $u = N_1(y)\delta u$ and $w = N_2(y)\delta w$, where $N_i(y)$ are the classical shape functions for a beam in bending.

The kinetic energy is attained from Eq. (3) which gives:

$$T_s = \frac{\rho S}{2}\int_0^L \left[\delta\dot{u}^t N_1^t N_1 \delta\dot{u} + \delta\dot{w}^t N_2^t N_2 \delta\dot{w}\right] dy + \frac{\rho I}{2}\int_0^L \left[\delta\dot{u}^t \frac{dN_1^t}{dy}\frac{dN_1}{dy}\delta\dot{u} + \delta\dot{w}^t \frac{dN_2^t}{dy}\frac{dN_2}{dy}\delta\dot{w}\right] dy$$
$$- 2\rho I\Omega \int_0^L \left[\delta\dot{u}^t \frac{dN_1^t}{dy}\frac{dN_2}{dy}\delta w\right] dy + \rho I L\Omega^2 \tag{26}$$

Replacing the shape functions (**??**) and (**??**) and their derivatives into Eq. (26) it is possible to reach the compact form:

$$T_s = \frac{1}{2}\delta\dot{u}^t M_1 \delta\dot{u} + \frac{1}{2}\delta\dot{w}^t M_2 \delta\dot{w} + \frac{1}{2}\delta\dot{u}^t M_3 \delta\dot{u} + \frac{1}{2}\delta\dot{w}^t M_4 \delta\dot{w} + \Omega\delta\dot{u}^t M_5 \delta w + \rho I L\Omega^2 \tag{27}$$

where matrices M_1 and M_2 are the classical mass matrices, M_3 and M_4 represent the rotational inertia effects and M_5 represents the gyroscopic effects. The last term, which is constant, will not present any contribution when Lagrange's equation is applied to (27) as follows:

$$\frac{d}{dt}\left(\frac{\partial T_s}{\partial \dot{\delta}}\right) - \frac{\partial T_s}{\partial \delta} = (M + M_s)\ddot{\delta} + C\dot{\delta} \tag{28}$$

where M and M_s are deduced directly from M_1, M_2, M_3 and M_4 and C from M_5. The matrices are:

$$C = \frac{\rho I \Omega}{15L}\begin{bmatrix} 0 & -36 & -3L & 0 & 0 & 36 & -3L & 0 \\ 36 & 0 & 0 & -3L & -36 & 0 & 0 & -3L \\ 3L & 0 & 0 & -4L^2 & -3L & 0 & 0 & L^2 \\ 0 & 3L & 4L^2 & 0 & 0 & -3L & -L^2 & 0 \\ 0 & 36 & 3L & 0 & 0 & -36 & 3L & 0 \\ -36 & 0 & 0 & 3L & 36 & 0 & 0 & 3L \\ 3L & 0 & 0 & L^2 & -3L & 0 & 0 & -4L^2 \\ 0 & 3L & -L^2 & 0 & 0 & -3L & 4L^2 & 0 \end{bmatrix} \quad \text{gyroscopic matrix} \tag{29}$$

$$M_s = \frac{\rho I}{30L}\begin{bmatrix} 36 & 0 & 0 & -3L & -36 & 0 & 0 & -3L \\ 0 & 36 & 3L & 0 & 0 & -36 & 3L & 0 \\ 0 & 3L & 4L^2 & 0 & 0 & -3L & -L^2 & 0 \\ -3L & 0 & 0 & 4L^2 & 3L & 0 & 0 & -L^2 \\ -36 & 0 & 0 & 3L & 36 & 0 & 0 & 3L \\ 0 & -36 & -3L & 0 & 0 & 36 & -3L & 0 \\ 0 & 3L & -L^2 & 0 & 0 & -3L & 4L^2 & 0 \\ -3L & 0 & 0 & -L^2 & 3L & 0 & 0 & 4L^2 \end{bmatrix} \quad \text{rotational inertia matrix} \tag{30}$$

$$M = \frac{\rho S L}{420}\begin{bmatrix} 156 & 0 & 0 & -22L & 54 & 0 & 0 & 13L \\ 0 & 156 & 22L & 0 & 0 & 54 & -13L & 0 \\ 0 & 22L & 4L^2 & 0 & 0 & 13L & -3L^2 & 0 \\ -22L & 0 & 0 & 4L^2 & -13L & 0 & 0 & -3L^2 \\ 54 & 0 & 0 & -13L & 156 & 0 & 0 & 22L \\ 0 & 54 & 13L & 0 & 0 & 156 & -22L & 0 \\ 0 & -13L & -3L^2 & 0 & 0 & -22L & 4L^2 & 0 \\ 13L & 0 & 0 & -3L^2 & 22L & 0 & 0 & 4L^2 \end{bmatrix} \quad \text{translational inertia matrix} \tag{31}$$

The strain energy of the shaft is obtained by means of Eq. (4) leading to:

$$U_s = \frac{EI}{2}\int_0^L \left[\delta u^t \frac{d^2 N_1^t}{dy^2}\frac{d^2 N_1}{dy^2}\delta u + \delta w^t \frac{d^2 N_2^t}{dy^2}\frac{d^2 N_2}{dy^2}\delta w\right] dy \tag{32}$$

After integration, the compact form is:

$$U_s = \frac{1}{2}\delta u^t K_1 \delta u + \frac{1}{2}\delta w^t K_2 \delta w \tag{33}$$

where K_1 and K_2 are the classical stiffness matrices.

It is frequently necessary to take into account the effect of shear, which will modify the classical stiffness matrix. The stiffness matrix with shear effects being taken into account is writen as:

$$K = \frac{EI}{(1+a)L^3}\begin{bmatrix} 12 & 0 & 0 & -6L & -12 & 0 & 0 & -6L \\ 0 & 12 & 6L & 0 & 0 & -12 & 6L & 0 \\ 0 & 6L & (4+a)L^2 & 0 & 0 & -6L & (2-a)L^2 & 0 \\ -6L & 0 & 0 & (4+a)L^2 & 6L & 0 & 0 & (2-a)L^2 \\ -12 & 0 & 0 & 6L & 12 & 0 & 0 & 6L \\ 0 & -12 & -6L & 0 & 0 & 12 & -6L & 0 \\ 0 & 6L & (2-a)L^2 & 0 & 0 & -6L & (4+a)L^2 & 0 \\ -6L & 0 & 0 & (2-a)L^2 & 6L & 0 & 0 & (4+a)L^2 \end{bmatrix} \tag{34}$$

In Eq. (34) a represents the effect of shear and is given by $a = (12EI)/(GS_r L^2)$. $S \approx S_r$ is the cross sectional area. If the shear effect is not to be taken into account, a must be set to zero.

3.3 Bearings

The bearings' stiffness and damping features are due to the displacements and velocities. The influence of angles and moments is usually not taken into account (Lalanne, 1996). Using Eq. (5) it is possible to achieve:

$$\begin{Bmatrix} F_u \\ F_w \\ F_\theta \\ F_\psi \end{Bmatrix} = -\begin{bmatrix} k_{xx} & k_{xz} & 0 & 0 \\ k_{zx} & k_{zz} & 0 & 0 \\ 0 & 0 & 0 & 0 \\ 0 & 0 & 0 & 0 \end{bmatrix}\begin{Bmatrix} u \\ w \\ \theta \\ \psi \end{Bmatrix} - \begin{bmatrix} c_{xx} & c_{xz} & 0 & 0 \\ c_{zx} & c_{zz} & 0 & 0 \\ 0 & 0 & 0 & 0 \\ 0 & 0 & 0 & 0 \end{bmatrix}\begin{Bmatrix} \dot{u} \\ \dot{w} \\ \dot{\theta} \\ \dot{\psi} \end{Bmatrix} \tag{35}$$

The first matrix is a stiffness matrix and second matrix a viscous damping matrix. These matrices are not usually symetric and the terms can vary as a function of the rotating speed.

3.4 Unbalance

The general kinetic energy expression due to unbalance is given by expression (7). The application of Lagrange's equation with $\delta = [u, w]^t$ gives:

$$\frac{d}{dt}\left(\frac{\partial T}{\partial \dot{\delta}}\right) - \frac{\partial T}{\partial \delta} = -m_u d\Omega^2 \begin{bmatrix} \sin\Omega t \\ \cos\Omega t \end{bmatrix} \tag{36}$$

3.5 Equations of motion

In building the global matrices, the elemental mass, damping, stiffness and force entries are then added to the corresponding rows and columns of the global mass, damping, stiffness and force matrices as in the following equation:

$$[M]\ddot{\delta} + [C(\Omega)]\dot{\delta} + [K]\delta = m_u d\sin\Omega t + m_u d\cos\Omega t \tag{37}$$

The elemental matrices can be added together to form the global matrices shown. The summation of the elemental matrices inside the global matrices must obey the order of the degrees of freedom in order to ensure the continuity of the whole structure.

3.6 Natural Frequencies and time Integration

For the calculation of natural frequencies the pseudo-modal method was used. In this method, the system matrices are reduced allowing the calculation of the first lower frequency natural frequencies without loss of accuracy. A modal space is defined from the solutions of:

$$[M]\ddot{\delta} + [K^*]\delta = 0 \tag{38}$$

where K^* is the actual stiffness matrix with supressed k_{xz} and k_{zx} terms in order to maintain simetry. The first $n << N$ modes $\phi_1 \ldots \phi_n$ are used to build a reduction matrix:

$$\phi = (\phi_1 \ldots \phi_n) \tag{39}$$

used for the change of base ($\delta = \phi p$). p is the vector of modal variables. The change of base is performed by premultiplying Eq. (37) by ϕ^t, leading to:

$$\phi^t M\phi\ddot{p} + \phi^t C(\Omega)\phi\dot{p} + \phi^t K\phi p = \phi^t F(t) \tag{40}$$

The transformed matrices ($m = \phi^t M\phi$, $c = \phi^t C(\Omega)\phi$, $k = \phi^t K\phi$, $f = \phi^t F(t)$) are then used to build a reduced equation of motion:

$$m\ddot{p} + c\dot{p} + kp = f \tag{41}$$

The natural frequencies are obtained by assuming a solution such as $p = Pe^{rt}$. Replacing this solution into Eq. (41) produces $[r^2 m + rc + k]p = 0$, which can be expressed as:

$$\begin{bmatrix} 0 & I \\ -k^{-1}m & -k^{-1}c \end{bmatrix} \begin{Bmatrix} rP \\ P \end{Bmatrix} = \frac{1}{r}\begin{Bmatrix} rP \\ P \end{Bmatrix} \tag{42}$$

The solution of the eigenproblem will produce complex conjugate frequencies that are modified as the value of Ω changes. The frequencies are in the form:

$$r_i = -\frac{\alpha_i\omega_i}{\sqrt{1-\alpha_i^2}} \pm j\omega_i \tag{43}$$

where α_i is also known as the damping factor. The orbits are obtained by the Newmark integration method.

4. Results

In this section the results for both methodologies are shown. Simulations with the twin-rotor simplified model of Coaracy Nunes power plant, shown in Fig. 1, were carried out considering a mass unbalance case, in the larger rotor, of 100 kg located at 2.5 m from its centre. The smaller rotor was considered with a mass unbalance of 50 kg located at 1.8 m from its centre.

4.1 Rayleigh-Ritz methodology

The Rayleigh-Ritz methodology made permitted the drawing of the Campbell diagram and the whirling orbits. The red line represents points on which the rotating frequency is equal to the natural frequency. The green line depicts the unbalance response. The blue lines represent the forward and backward natural frequencies of the system.

The unbalance response was plotted in the same figure as the Campbell Diagram. One can note that the peak amplitude is located at the same rotational speed of the first critical speed which is 1000 rpm. The rotational speed of the assembly is 150 rpm which assures safety against resonance. If anisotropic bearings were to be considered, the two curves (in blue) would separate at $\Omega = 0$ rpm and the green curve would show two peaks with the second peak coinciding with the second critical speed.
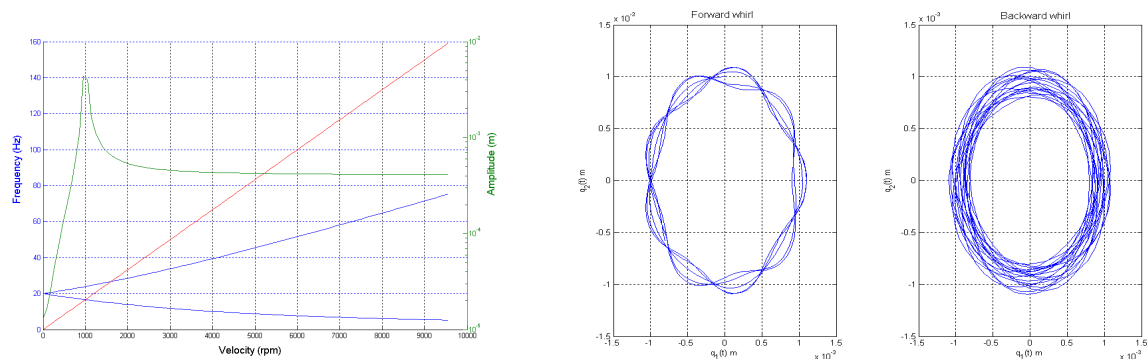

Figure 2. Campbell Diagram for Coaracy Nunes assembly showing unbalance response and Forward and Backward whirl orbits

The orbits for the Rayleigh-Ritz simulation were obtained by means of a fourth order Runge-Kutta integration procedure. The forward and backward configurations can be achieved by changing the initial conditions for each generalized displacement and speed. The whirling orbit for forward and backward whirl in the unbalanced cases are shown in Fig. 2.

4.2 The Finite Element methodology

For the Finite Element method, the evolution of natural frequencies with the increase of rotational speed was obtained by means of an eigenvalue procedure of a system including a damping matrix. As a result, all the frequencies obtained are of complex form. The mode frequencies plotted in the Campbell diagram are complex conjugate frequencies as shown in Fig. (3). The corresponding unbalance response is also shown with the Campbell Diagram.
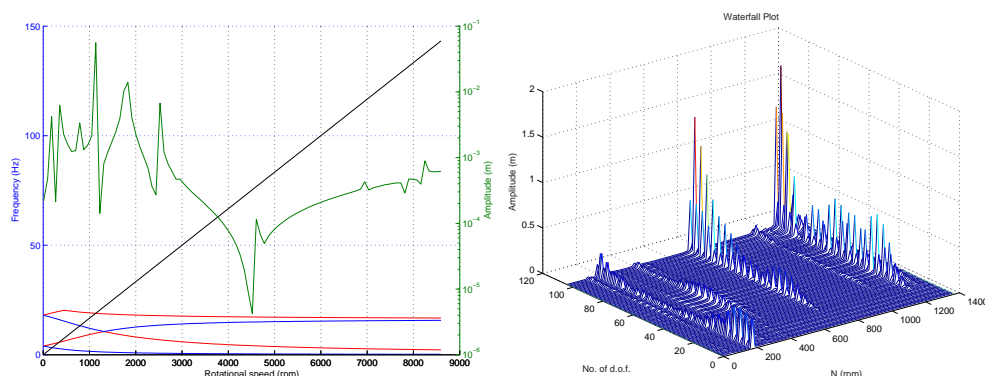

Figure 3. Forward and backward whirl frequencies plotted with unbalance response and waterfall FRF plot for the unbalanced response

The first four critical speeds of Fig. (3) are $193.8\ rpm$, $336\ rpm$, $801.6\ rpm$ and $1142.4\ rpm$. It is interesting to visualize the unbalance response for the Coaracy Nunes assembly on all of its degrees of freedom. This can be achieved as shown in Fig. (3) where a waterfall plot is drawn. The waterfall plot is capable of showing the amplitude values of each degree of freedom varying with the rotational speed. The whirling orbit obtained shows a pathline that is not as circular as the one obtained for the Rayleigh-Ritz methodology. This feature is a result of the initial conditions necessary for each degree of freedom. In this case, the displacement initial condition was the first natural static mode shape with frequency of 1089 rad/s (5.25 Hz). The velocity initial condition was the first mode shape multiplied by its frequency.

Figure (4) shows the forward whirl orbit of one of the axis degrees of freedom and the 3D whirling orbits of all the system displacement degrees of freedom.
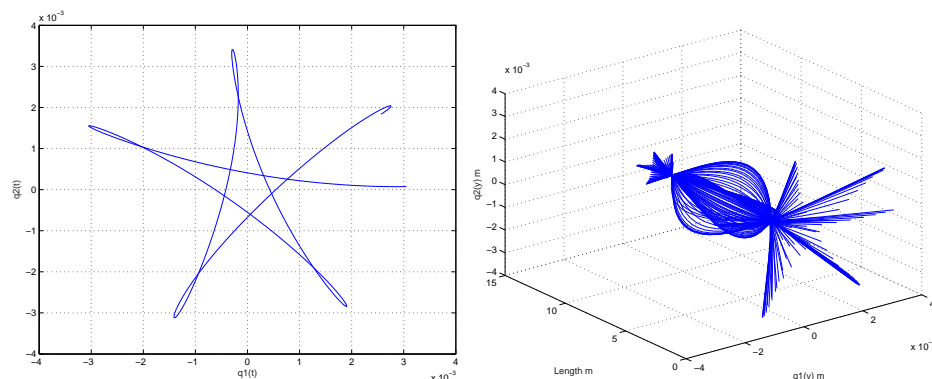

Figure 4. 2D and 3D forward whirl orbits

5. Final remarks

This work presented the use of classical methodologies in the rotordynamic analysis of a hydro turbine rotor-generator assembly. To this end, the Rayleigh-Ritz methodology was applied in order to obtain a general direction for the Finite Element procedure. Due to the use of few degrees of freedom the Rayleigh-Ritz results allowed a better understanding of the general behavior of the rotor-generator assembly through the assessment of the evolution of its natural frequencies with the increase of rotational speed. The response due to unbalanced conditions was applied to confirm the critical speed obtained with the Campbell diagram. The whirling orbit obtained showed an approximate circular orbit which indicates that the shaft is rotating in its own natural frequency speed.

The routines built for the Finite Element analysis present a general scope of applications and can be used in the analysis of many rotordynamics problems taking into account, naturally, their level of simplicity. The use of Timoshenko beam elements is particularly interesting due to the inclusion of shear effects into the stiffness matrix.

The use of classical and traditional methodologies in the analysis of a simplified model of complex structures is extremely important because it will supply valuable information necessary in the analysis of the same problem using commercial packages and more complex geometries. This comprehensive approach will allow the assessment of mode shapes and natural frequencies that are already known at some extent. Hence, errors due to lack of information about the natural physical behavior of such structure will be greatly diminished.

6. References

Betting, B., 2000, "Rotordynamics", Notes on website http://www.me.mtu.edu/ mdrl, Michigan Technological University, Michigan, USA.

Géradin, M., Rixen, D., 1997, "Mechanical Vibrations, Theory and Application to Structural Dynamics", John Wiley & Sons, Chichester, England, 425 p.

Hoffman, J. D., 2001, "Numerical Methods for Scientists and Engineers", Marcel Dekker, New York, 823 p.

Krodkiewski, J. M., 2002, "Dynamics of Rotors", Course Material, University of Melbourne, Department of Mechanical and Manufacturing Engineering, Melbourne, Australia.

Lalanne, M., Ferraris, G., 1990, "Rotordynamics Prediction in Engineering", John Wiley & Sons, London, England, 198 p.

Lalanne, M., Ferraris, G., 1996, "Dynamique des Rotors en Flexion", Results of research problems, Institut National des Sciences Appliquées (INSA) de Lyon, Lyon, France.

Meirovitch, L., 1986, "Elements of Vibration Analysis", McGraw Hill, New York, USA, 560 p.

Pereira, J. C., 2003, "Introdução à Dinâmica de Rotores", Lecture Notes, Universidade Federal de Santa Catarina, Departamento de Engenharia Mecânica, Florianópolis, Brasil.

Vinaud, F.J., Diniz, C.G.C., 2004, "Comparação de Métodos para Estudo dinâmico de Hidrogeradores", Anais do VI Simpósio Mineiro de Mecânica Computacional, Itajubá, Brasil.

Vinaud, F.J., Diniz, C.G.C., 2005, "Use of Simplified Models in the Dynamic Study of Hydrogenerators", Proceedings of the XI DINAME, Ouro Preto, Brasil.

7. Responsibility notice

The author(s) is (are) the only responsible for the printed material included in this paper